

Electromagnetic Transients of a Micro-Turbine Based Distributed Generation System

H. Nikkhajoei, *Member, IEEE*, R. Iravani, *Fellow, IEEE*

Abstract—This paper evaluates the electromagnetic transients of a micro-turbine based distributed generation system that includes an AC-DC-AC converter. An outline of modelling the micro-turbine based generation system including the AC-DC-AC converter is presented. A controller for the converter, that consists of a number of single-input single-output sub-controllers, is designed based on the developed model of the system. Furthermore, the thermodynamic model of micro-turbine system is presented. The electromagnetic transients of the overall micro-turbine based generation system including the micro-turbine and converter controllers are evaluated based on time-domain simulation studies in the PSCAD/EMTDC software environment. The study considers the dynamic models of generator, converter and power system and the thermodynamic model of micro-turbine system.

Index Terms—Electromagnetic Transient, Micro-Turbine Generator, Distributed Generation, Dynamic Model, AC-DC-AC Converter, Control Design, Thermodynamics.

I. INTRODUCTION

THE Micro-Turbine Generator (MTG) has emerged as a viable source of electric energy in the context of Distributed Generation (DG) [1]-[3]. It can also provide power demand for remote military/commercial applications, as a stand-alone generator unit. An MTG unit is usually a high-speed (up to 120 krpm) rotating machine with the output power of up to a few hundreds of kilowatts, and the output frequency of higher than 50/60 Hz (e.g. 400 Hz and up to several kHz). Thus, it is interfaced through a power electronic converter to the load/utility system. The converter provides conversion/control of frequency as well as control of the output voltage and power flow of the MTG-converter module. Different types of AC-AC conversion systems, e.g. matrix converter [4], [8] or AC-DC-AC converter, can be adopted as the power electronic interface of an MTG unit. However, the AC-DC-AC based configuration is conventionally used for the MTG unit [5]-[7]. In this configuration, the MTG-side converter is either a diode-rectifier, a thyristor-rectifier or a Voltage-Sourced Converter (VSC) and the utility side converter is often a VSC unit, Fig. 1.

The main focus of this paper is to study the electromagnetic transient behavior of an AC-DC-AC based MTG system. This paper also presents a detailed dynamic model of the overall system that is used to design a controller for the AC-DC-AC

converter. The model is based on transformation of the system equations to a Switching Reference Frame (SRF) [4] and then to the dqo reference frame. The dqo reference frame is selected such that the operating parameters of system can be independently controlled. As a result, the multi-input multi-output converter system is decomposed to a number of Single-Input Single-Output (SISO) sub-systems. For each subsystem, a SISO controller is systematically designed.

The thermodynamic behavior of micro-turbine system is addressed in this paper and the corresponding thermodynamic model is presented. Based on this model, a fast response controller is designed for the micro-turbine system. The thermodynamic model is incorporated in the dynamic model of the MTG system since thermodynamics of the high-speed micro-turbine has a fairly small time constant which is comparable to that of the electromagnetic transients of a 50/60 Hz power system [4], [8]. The electromagnetic transient behavior of the overall MTG system including the designed controllers is evaluated based on digital time-domain simulation studies.

II. CONVERTER MODEL

Fig. 1 shows schematic diagram of a back-to-back VSC that interfaces two AC systems with nominal frequencies of ω_i and ω_o . The AC systems are referred to as source-side and network-side systems, and are simplified representations of a micro-turbine generator and a utility distribution system, respectively.

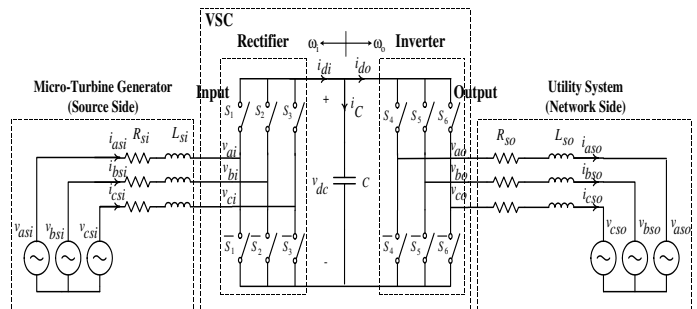


Fig. 1. Schematic representation of two AC systems interfaced by a back-to-back VSC

A. Switching Reference Frame based Model

The theoretical concept of Switching Reference Frame (SRF) is introduced in [4], [8]. For a back-to-back VSC, transformation to the SRF for the rectifier module, Fig. 1, is defined by

$$F_i^s = S_R F_{si}, \quad (1)$$

H. Nikkhajoei and R. Iravani are with the Center for Applied Power Electronics (CAPE), Department of Electrical and Computer Engineering, University of Toronto, 10 King's College Road, Toronto, Ontario M5S 3G4, Canada. E-mails: h.nikkhajoei@utoronto.ca, iravani@ecf.utoronto.ca

where

$$F_i^s = [f_{ai}^s \ f_{bi}^s \ f_{ci}^s \ f_{di}]^T \quad (2)$$

$$F_{si} = [f_{asi} \ f_{bsi} \ f_{csi} \ f_{dc}]^T \quad (3)$$

$$S_R = \begin{bmatrix} 0 & 0 & 0 & S_1 - \frac{1}{3} \\ 0 & 0 & 0 & S_2 - \frac{1}{3} \\ 0 & 0 & 0 & S_3 - \frac{1}{3} \\ \frac{3}{2}S_1 & \frac{3}{2}S_2 & \frac{3}{2}S_3 & 0 \end{bmatrix}. \quad (4)$$

S_1 , S_2 and S_3 are the switching functions of the switches of the rectifier module. In (2) and (3), f represents an electrical quantity, e.g. voltage or current, the subscripts ‘‘i’’ and ‘‘si’’ represent quantities related to the converter input side and the source, respectively, and superscript ‘‘s’’ denotes quantities transformed to the SRF. f_{dc} represents a DC-link quantity and f_{di} is the equivalent quantity in the SRF. For the inverter module, Fig. 1, a set of equations similar to (1)-(4) can be written.

The voltage equation related to the source-side circuit of converter, Fig. 1, is

$$v_{abcsi} = R_i i_{abcsi} + L_i p(i_{abcsi}) + v_{abci}, \quad (5)$$

where p is the $\frac{d}{dt}$ operator, $R_i = \text{diag}\{R_{si}, R_{si}, R_{si}\}$, $L_i = \text{diag}\{L_{si}, L_{si}, L_{si}\}$ and

$$v_{abcsi} = [v_{asi} \ v_{bsi} \ v_{csi}]^T \quad (6)$$

$$i_{abcsi} = [i_{asi} \ i_{bsi} \ i_{csi}]^T \quad (7)$$

$$v_{abci} = [v_{ai} \ v_{bi} \ v_{ci}]^T. \quad (8)$$

Transferring (5) to the SRF based on (1), we deduce

$$v_{di} = \frac{3}{2}R_{si}i_{di} + \frac{3}{2}L_{si}p(i_{di} - i_{di0}) + v_{dc}, \quad (9)$$

where v_{di} and i_{di} are equivalents of the voltage and current of the source v_{abcsi} in the SRF. Similarly, for the network-side circuit of Fig. 1, the voltage equation transferred to the SRF is

$$v_{do} = -\frac{3}{2}R_{so}i_{do} - \frac{3}{2}L_{so}p(i_{do} - i_{do0}) + v_{dc}, \quad (10)$$

where v_{do} and i_{do} are equivalents of the voltage and current of the source v_{abcs0} in the SRF.

B. System Model in dqo Frame

Since the dynamic model of an electrical system is traditionally developed in the dqo rotating reference frame, it is desirable to obtain the model of system of Fig. 1 in the dqo frames of the source and network sides. To transfer the source (network) side variables to the dqo frame, a transformation matrix is selected such that the d and q components of source (network) current are proportional to the corresponding real and reactive power components. Thus, control of each current component regulates the corresponding power component.

The converter source-side variables are transferred to the dqo frame by

$$f_{qdoi}^s = K_i^s f_{abci}, \quad (11)$$

where the transformation matrix K_i^s is

$$K_i^s = \frac{2}{3} \begin{bmatrix} \cos \theta_i & \cos(\theta_i - \frac{2\pi}{3}) & \cos(\theta_i + \frac{2\pi}{3}) \\ \sin \theta_i & \sin(\theta_i - \frac{2\pi}{3}) & \sin(\theta_i + \frac{2\pi}{3}) \\ \frac{1}{2} & \frac{1}{2} & \frac{1}{2} \end{bmatrix}, \quad (12)$$

$$\theta_i(t) = \int_0^t \omega_i(t)dt + \alpha_i(0). \quad (13)$$

α_i is phase-angle of the source phase-a voltage, i.e. v_{asi} . Assume that the switching functions S_1 , S_2 and S_3 , Fig. 1, are approximated with their fundamental components as

$$\begin{bmatrix} S_1(t) \\ S_2(t) \\ S_3(t) \end{bmatrix} = A_{mi} \begin{bmatrix} \sin \theta_{mi}(t) \\ \sin(\theta_{mi}(t) - \frac{2\pi}{3}) \\ \sin(\theta_{mi}(t) + \frac{2\pi}{3}) \end{bmatrix}, \quad (14)$$

where $\theta_{mi}(t) = \omega_i t + \alpha_{mi}$. A_{mi} and α_{mi} are the amplitude and angle modulation indices of the rectifier module, Fig. 1. The transformed version of source-side abc variables of Fig. 1 to the corresponding dqo frame, based on (5), (11) and (14), is

$$v_{msi} \begin{bmatrix} 0 \\ 1 \\ 0 \end{bmatrix} = R_i i_{qdoi}^s + L_i p(i_{qdoi}^s) + \omega_i \begin{bmatrix} 0 & 1 & 0 \\ -1 & 0 & 0 \\ 0 & 0 & 0 \end{bmatrix} L_{si} i_{qdoi}^s + \frac{1}{2} A_{mi} v_{dc} \begin{bmatrix} \sin(\alpha_{mi} - \alpha_i) \\ \cos(\alpha_{mi} - \alpha_i) \\ 0 \end{bmatrix}, \quad (15)$$

where v_{msi} and v_{dc} are the amplitude of source voltage and the DC-link voltage, respectively. Similarly, for the network side circuit of Fig. 1, it can be shown that

$$-v_{mso} \begin{bmatrix} 0 \\ 1 \\ 0 \end{bmatrix} = R_o i_{qdos0}^s + L_o p(i_{qdos0}^s) + \omega_o \begin{bmatrix} 0 & 1 & 0 \\ -1 & 0 & 0 \\ 0 & 0 & 0 \end{bmatrix} L_{so} i_{qdos0}^s - \frac{1}{2} A_{mo} v_{dc} \begin{bmatrix} \sin(\alpha_{mo} - \alpha_o) \\ \cos(\alpha_{mo} - \alpha_o) \\ 0 \end{bmatrix}. \quad (16)$$

In (16), v_{mso} and α_o are the magnitude and angle of the source phase-a voltage, i.e. v_{aso} , and A_{mo} and α_{mo} are the amplitude and angle modulation indices of the inverter module, Fig. 1.

For the DC-link circuit of Fig. 1, we have

$$p(v_{dc}) = \frac{1}{C}(i_{di} - i_{do}), \quad (17)$$

where

$$i_{di} = \frac{3}{4} A_{mi} [i_{qsi}^s \sin(\alpha_{mi} - \alpha_i) + i_{dsi}^s \cos(\alpha_{mi} - \alpha_i)] \quad (18)$$

$$i_{do} = \frac{3}{4} A_{mo} [i_{qso}^s \sin(\alpha_{mo} - \alpha_o) + i_{dso}^s \cos(\alpha_{mo} - \alpha_o)]. \quad (19)$$

The dqo -based model of the system of Fig. 1 is given by (15), (16) and (17). Based on this mathematical model, the system of Fig. 1 can be represented by the equivalent circuits of Fig. 2.

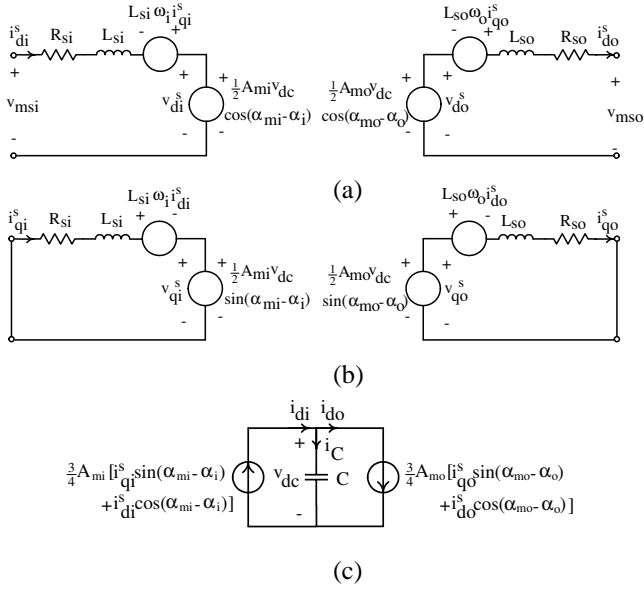


Fig. 2. Dqo reference frame-based model of the system of Fig. 1: (a) d -axis and (b) q -axis equivalent circuits of source/network sides, (c) DC-link equivalent circuit

III. CONVERTER CONTROL

For the system of Fig. 1, the back-to-back VSC can be controlled based on the dqo model of the system shown in Fig. 2. The voltage equations of the source-side system, based on the equivalent circuits of Fig. 2, are

$$v_{di}^s = v_{msi} - R_{si}i_{dsi}^s - L_{si}p(i_{dsi}^s) + L_{si}\omega_i i_{qsi}^s \quad (20)$$

$$v_{qi}^s = -R_{si}i_{qsi}^s - L_{si}p(i_{qsi}^s) - L_{si}\omega_i i_{dsi}^s, \quad (21)$$

where v_{di}^s and v_{qi}^s are the d - and q -axis components of the terminal voltage of the rectifier module, respectively, Fig. 2. To have a simple control system for the converter, a set of intermediate variables is selected such that the real and reactive power components at the source (network) side are independently controlled. As a result, the multi-input multi-output converter system can be controlled by a number of SISO sub-controllers. The stability of each sub-system guarantees the stability of overall multi-variable system [9]. To simplify the control system, the derivatives of the current components i_{di}^s and i_{qi}^s are defined, based on (20) and (21), as

$$p(i_{dsi}^s) = -\frac{R_{si}}{L_{si}}i_{dsi}^s + dv_{di} \quad (22)$$

$$p(i_{qsi}^s) = -\frac{R_{si}}{L_{si}}i_{qsi}^s + dv_{qi}, \quad (23)$$

where

$$dv_{di} = \omega_i i_{qsi}^s - \frac{v_{di}^s - v_{msi}}{L_{si}} \quad (24)$$

$$dv_{qi} = -\omega_i i_{dsi}^s - \frac{v_{qi}^s}{L_{si}}. \quad (25)$$

For dv_{di} and dv_{qi} given by (24) and (25), the current components i_{dsi}^s and i_{qsi}^s are fictitiously decoupled based on (22) and (23) and, therefore, can be independently controlled. Based on

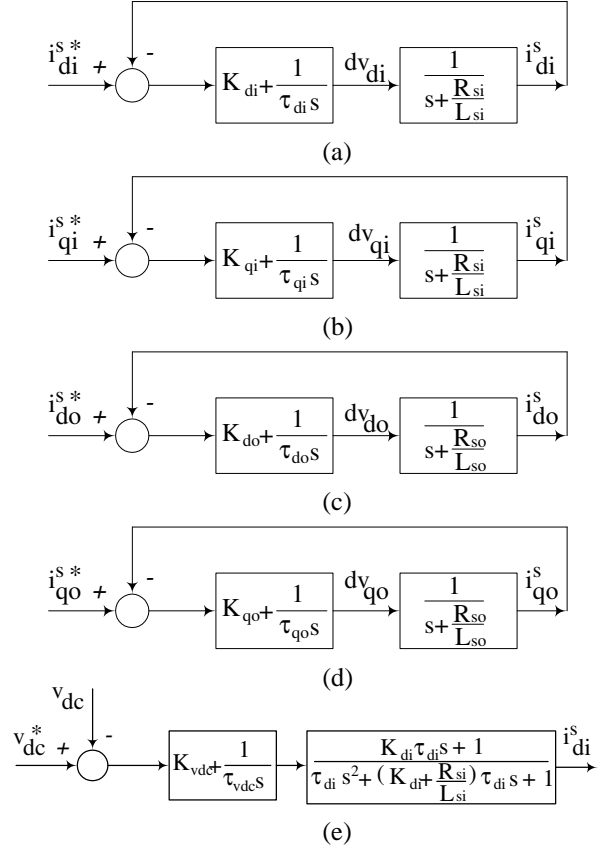


Fig. 3. SISO sub-controllers for the system of Fig. 1: (a),(b) source real/reactive current components, (c),(d) network real/reactive current components, (e) DC-link voltage

(20) and (21), the voltage components v_{di}^s and v_{qi}^s in terms of dv_{di} and dv_{qi} and the current components i_{dsi}^s and i_{qsi}^s are

$$v_{di}^s = v_{msi} - R_{si}i_{dsi}^s - L_{si}dv_{di} + L_{si}\omega_i i_{qsi}^s \quad (26)$$

$$v_{qi}^s = -R_{si}i_{qsi}^s - L_{si}dv_{qi} - L_{si}\omega_i i_{dsi}^s. \quad (27)$$

For the network-side circuit of Fig. 1, equations similar to (22)-(27) can be obtained based on the d - and q -axis representation of the circuit shown in Fig. 2. Based on the mathematical model of (22)-(27) and that of the network-side circuit, the system of Fig. 1 is decomposed to a number of SISO sub-systems that are shown in Fig. 3. Based on these SISO sub-systems, each PI controller represented by the left-side block, Fig. 3, is designed using MATLAB SISO tools, where the system parameters are given in Appendix A. Table I lists the proportional/integrating parameters of the five PI controllers shown in Fig. 3. The controller of the DC-link voltage is designed based on the SISO sub-system of Fig. 3(e). The transfer function of this sub-system is the resultant block of the system of Fig. 3(a) that relates i_{dsi}^{s*} to i_{dsi}^s .

TABLE I: PARAMETERS OF THE PI CONTROLLERS

PI Controller	Gain	Time Constant (ms)
Fig. 3(a)	11000	20
Fig. 3(b)	11000	20
Fig. 3(c)	1450	0.8
Fig. 3(d)	1450	0.8
Fig. 3(e)	200	0.5

When the values of variables dv_{di} , dv_{qi} , dv_{do} and dv_{qo} are calculated based on Figs. 3(a)-(d), the settings of converter modules, i.e. A_{mi} , α_{mi} , A_{mo} and α_{mo} , can be obtained. For instance, the settings of the rectifier module are calculated from

$$A_{mi} = \frac{2}{v_{dc}} \sqrt{(v_{di}^s)^2 + (v_{qi}^s)^2} \quad (28)$$

$$\alpha_{mi} = \tan^{-1}\left(\frac{v_{qi}^s}{v_{di}^s}\right) + \alpha_i, \quad (29)$$

where v_{di}^s and v_{qi}^s are obtained from (26) and (27) for given values of dv_{di} and dv_{qi} .

IV. MICRO-TURBINE GENERATOR

The MTG unit is composed of a high-speed (up to 120 krpm) gas turbine and a permanent-magnet synchronous (PMS) generator. The turbine includes the three compartments of compressor, combustion chamber and turbine. Fundamentals of operation and details of the compartments of a gas turbine can be found in [8], [10].

A micro-turbine has much smaller physical dimensions than a conventional gas turbine. The length of each compartment of a micro-turbine is relatively short and gas moves at a relatively fast speed, e.g. $100 \frac{m}{s}$ [11], inside the micro-turbine compartments. Hence, each compartment of a micro-turbine has a small thermodynamic time constant, e.g. 1.5 ms, [11]. Thus, any change in the input fuel or the air flow of a micro-turbine affects its output mechanical power in a short period of time. Therefore, thermodynamics of the micro-turbine should be considered in the analysis of the dynamic performance of an MTG unit, and the input mechanical power to the generator can not be considered as a constant value during electromechanical dynamics of the generator.

A. Micro-Turbine Control

A block diagram representing the operation of a micro-turbine system is shown in Fig. 4(a). The thermal behaviors of the compartments are quantified by the parameter k_p and the temperatures T_a , T_c , T_{cc} and T_T . The thermal power of the compressor $P_{th,c}$ changes its output power with a time constant of τ_c . The micro-turbine inputs, Fig. 4(a), are the air and fuel mass flow rates. The mass flow rate of the fuel is proportional to that of the air [8]. Hence, the air mass flow rate can be considered as the input of a micro-turbine. The output is the mechanical power $P_m(t)$ which is delivered to the generator [8].

In an MTG unit, to control the electrical power of the generator, the output mechanical power of the micro-turbine is controlled. The block diagram of the micro-turbine controller is shown in Fig. 4(b). It includes a PI controller to regulate the input air mass flow rate based on the command of the output mechanical power. The controller of Fig. 4(b) also includes a feedback signal from the generator speed to adjust it to the desired reference speed ω_m^* . The controller inputs are the reference values of speed (ω_m^*) and power (P_m^*) and the corresponding measured values, i.e. ω_m and P_m . The scaling factors of speed and power are $k_1 = 14.33$ and $k_2 = 1$, respectively. The input of the PI controller is the summation of the scaled errors and

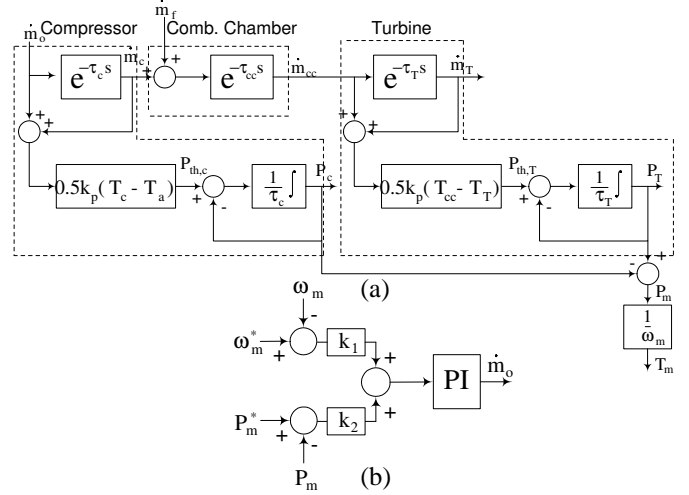


Fig. 4. (a) Block diagram of micro-turbine system (b) Micro-turbine controller

the output is the reference of the air mass flow rate \dot{m}_o which is given as the input to the micro-turbine system. The parameters of the micro-turbine system of Fig. 4(a) is given in Table II. The parameters of the PI controller of Fig. 4(a) are $k = 500$ and $\tau = 0.1$ ms.

TABLE II: PARAMETERS OF MICRO-TURBINE SYSTEM

Compressor time constant, τ_c	13 ms
Combustion chamber time constant, τ_{cc}	14 ms
Turbine time constant, τ_T	0.294 ms
Ambient temperature, T_a	25 °C
Compressor outlet temperature, T_c	210 °C
Combustion chamber outlet temp., T_{cc}	982 °C
Turbine outlet temperature, T_T	315 °C
Heat capacity constant of gas, k_p	470.39

V. PERFORMANCE OF MTG SYSTEM

This section investigates the closed-loop performance of the overall MTG system including the power and control subsystems as depicted in Fig. 5. The system of Fig. 5 considers a micro-turbine generator in the place of the simplified representation of the generator, Fig. 1, that was used specifically for modelling of system and design of a controller for the converter. In the system of Fig. 5, the micro-turbine is represented by its thermodynamic model of Fig. 4(a). The generator is a permanent-magnet, synchronous machine which is represented in its d-q frame with two windings on each axis [12]. The generator is rated at 100 kW, 600 V and its rated output frequency is 2221 Hz. The converter is represented by the circuit shown in Fig. 5 and the converter switches are modelled as ideal on-off switches. The conventional sinusoidal PWM strategy of is used to turn the switches on and off. The utility system is modelled as a three-phase ideal voltage source in series with an R-L branch in each phase. The converter control is represented by the block diagrams of Figs. 3(a) to (e). The micro-turbine and its control are represented by the block diagrams of Figs. 4(a) and 4(b). The studies presented in this section are conducted in time-domain in the PSCAD/EMTDC software environment.

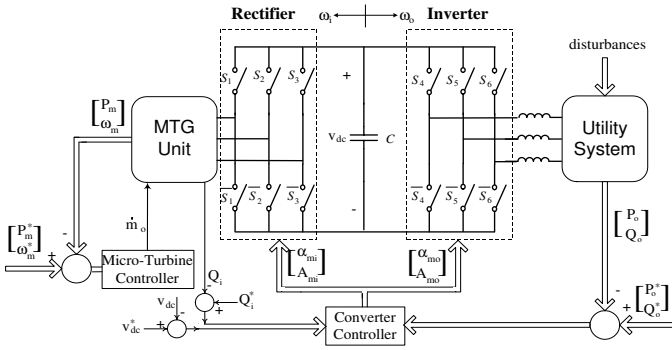


Fig. 5. The overall study system including the power and control sub-systems.

A. Transient Response to a Control Command

Fig. 6 shows the transient response of the system of Fig. 5 to a step change in the reactive power demand of the utility system. Initially the system is under a steady-state condition and supplies almost no reactive power to the utility system at its terminal. At $t=0.1$ s, the reactive power command, Q_o^* , is changed from 0 to -0.5 pu. Fig. 6(a) shows variations in the reference i_{qo}^{s*} , associated with Q_o^* , and i_{qo}^s . Fig. 6(b) indicates that although the real power command i_{do}^{s*} remains unchanged, i_{do}^s is temporarily changed and the real power controller, Fig. 3(c), forces i_{do}^s to track the initial set value. Figs. 6(c) and (d) show the dynamics in the generator speed and electromagnetic torque in response to the command change. Figs. 6(e) to (h) show changes in of the amplitude and angle modulation indices of the rectifier and inverter modules in response to the change of system commands.

B. Transient Response to a Fault

Fig. 7 shows transient response of the system of Fig. 5 to a phase-to-phase short-circuit fault at the converter source-side terminals. The fault occurs at $t=0.1$ s and is cleared after 50 ms. Figs. 7(a) and (b) show variations of the real and reactive components of utility current during and after the fault. Figs. 7(c) and (d) show variations of the reactive component of generator current and the DC-link voltage due to the short-circuit fault. Figs. 7(e) and (f) show changes of the generator speed and electromagnetic torque in response to the fault.

VI. CONCLUSIONS

This paper evaluates the electromagnetic transient behavior of a high-speed micro-turbine generation system which is interfaced to a utility system by a back-to-back converter. The paper also develops the dynamic model of the overall system, including the models of the converter and micro-turbine systems. The converter dynamic model is used to design a controller for the converter based on a systematic approach. Furthermore, the thermodynamic behavior of the micro-turbine is addressed and, based on the turbine thermodynamic model, a controller is designed for the micro-turbine system. The presented results show that the designed controllers for the converter and micro-turbine systems ensure desirable performance and stability of the overall micro-turbine generation system as a distributed generation unit.

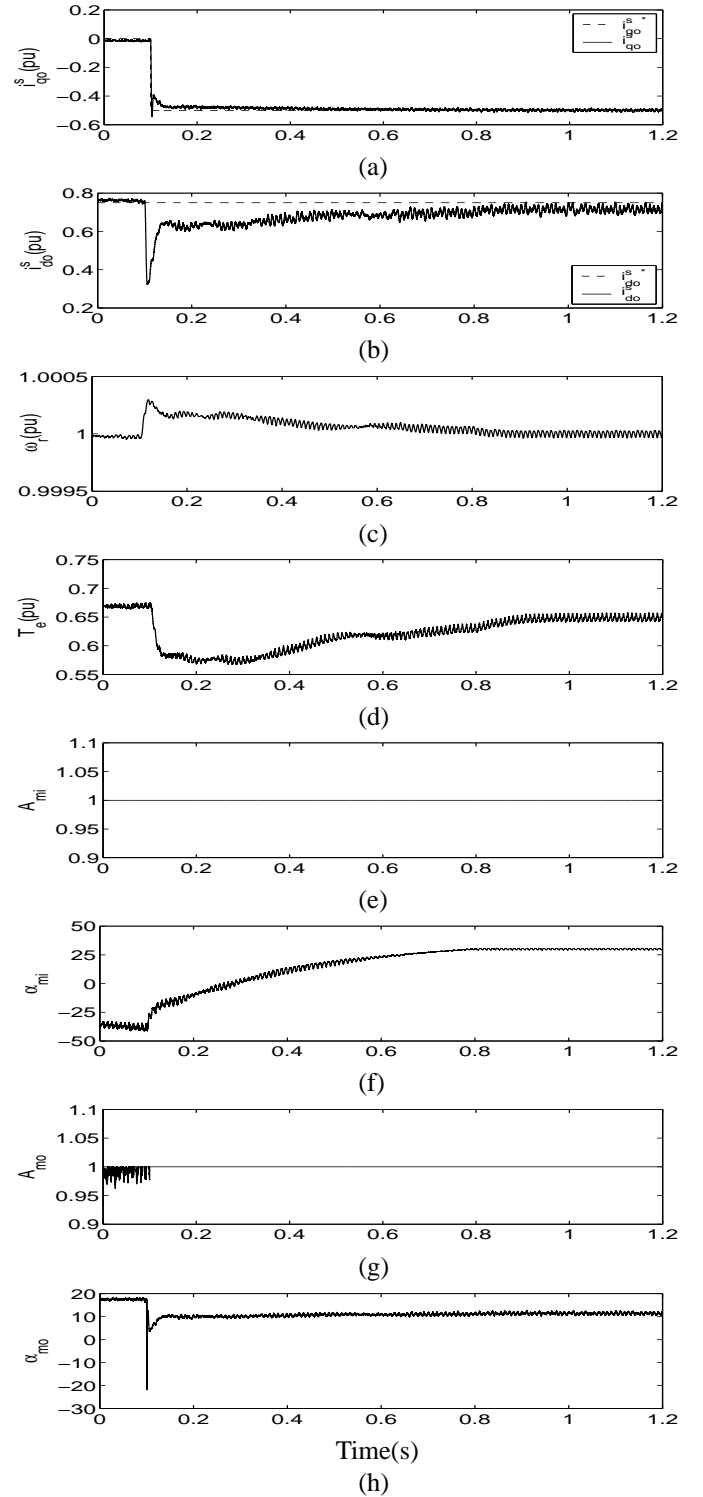


Fig. 6. Transient Response of the system of Fig. 5 to a step change in the reactive component of utility current: (a) q-axis and (b) d-axis components of utility system current, (c) generator speed, (d) electromagnetic torque, and amplitude and angle modulation indices of rectifier ((e),(f)) and inverter ((g),(h)) modules

VII. APPENDIX A: SYSTEM PARAMETERS

The parameters of the system of Fig. 1 are listed in Table III. The base values of the system power and the source/network side line voltages are, respectively, $S_b = 100$ kVA, $V_{bi} = 600$ V and $V_{bo} = 600$ V.

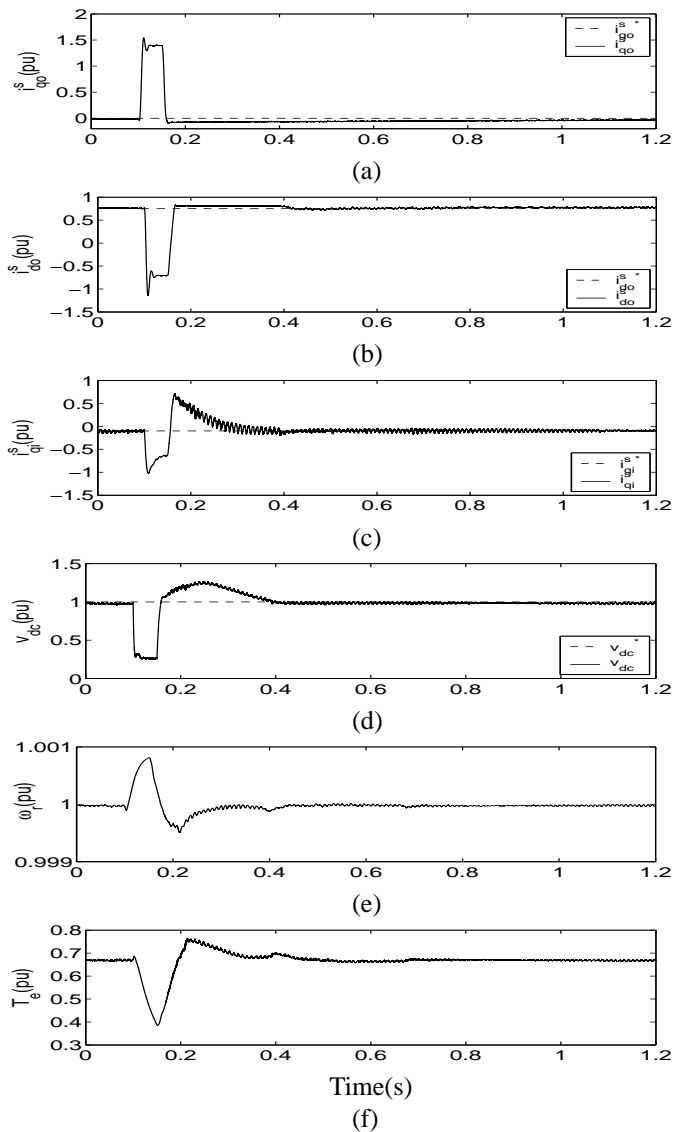


Fig. 7. Transient Response of the system of Fig. 5 to a phase-to-phase short circuit at the converter source-side terminals: (a) q-axis and (b) d-axis components of utility system current, (c) q-axis component of generator current, (d) DC-link voltage, (e) generator speed, and (f) electromagnetic torque

TABLE III: PARAMETERS OF THE SYSTEM OF FIG. 1

Source-Side Parameters	
Source rated power	1.0 pu
Source voltage, v_i	1.0 pu
Source frequency, f_i	2221 Hz
Source resistance, R_{si}	0.014 pu
Source reactance, X_{si}	0.969 pu
Rectifier switching frequency, f_{swi}	20 kHz
Network-Side Parameters	
Network voltage, v_o	1.0 pu
Network frequency, f_o	60 Hz
Network resistance, R_{so}	0.167 pu
Network reactance, X_{so}	0.628 pu
Inverter switching frequency, f_{swo}	1860 Hz
DC-link Capacitor, C	1000 μ F

REFERENCES

- [1] F. R. Goodman, E. P. Dick, G. R. Berube, L. M. Hajagos, R. J. Marttila, and R. D. Quick, "Integration of distributed resources in electric utility distribution systems; distribution system behavior analysis for suburban feeder," *EPRI and Ontario Hydro Technologies*, Final report, November 1998.
- [2] M. W. Davis, A. H. Gifford, and T. J. Krupa, "Microturbines-an economic and reliability evaluation for commercial, residential, and remote load applications," *Proc. IEEE Power Engineering Society Winter Meeting*, Vol. 2, pp. 888-888, February 1999.
- [3] S. Hamilton, "Fuel cell-MTG hybrid the most exciting innovation in power in the next 10 years," *Proc. IEEE Power Engineering Society Summer Meeting*, Vol. 1, pp. 581-588, July 1999.
- [4] H. Nikkhajoei, A. Tabesh, and R. Iravani, "Dynamic model of a matrix converter for controller design and system studies," *Resubmitted, with minor revision, for publication in IEEE Trans. on Power Delivery*.
- [5] D. Casadei, G. Grandi, R. K. Jordan, and F. Profumo, "Control strategy of a power line conditioner for cogeneration plants," *Proc. IEEE-PESC'99*, Vol. 2, pp. 607-612, June 1999.
- [6] D. Casadei, G. Grandi, and C. Rossi, "Effects of supply voltage non-idealities on the behavior of an active power conditioner for cogeneration systems," *Proc. IEEE-PESC'00*, Vol. 3, pp. 1312-1317, June 2000.
- [7] R. K. Jordan, I. Nagy, T. Nita, and H. Ohsaki, "Environment-friendly utilisation of waste energies for the production of electric energy in disperse power plants," *Proc. ISIE Int'l Symposium on Industrial Electronics*, Vol. 4, pp. 1119-1124, July 2002.
- [8] H. Nikkhajoei, "Matrix converter and its application in a micro-turbine based generation system," Ph.D. dissertation, University of Toronto, 2004.
- [9] J. M. Maciejowski, "Multivariable Feedback Design," *Addison-Wesley Publishing Company*, 1989.
- [10] P. P. Walsh and P. Fletcher, "Gas turbine performance", *Blackwell Science Publications*, 1998.
- [11] H. J. Nern, H. Kreshman, F. Fischer, and H. A. Nour Eldin, "Modelling of the long term dynamic performance of a gas turbo generator set," *Proc. IEEE Conf. on Control Applications*, Vol. 1, pp. 491-496, August 1994.
- [12] P. C. Krause, "Analysis of electric machinery", *McGraw-Hill Publications*, 1986.



Hassan Nikkhajoei (M'2005) received the B.Sc. and M.Sc. degrees from Isfahan University of Technology, Isfahan, Iran, in 1992 and 1995, respectively, and Ph.D. degree from the University of Toronto, Toronto, Canada in 2004, all in electrical engineering. He was a faculty member at the Department of Electrical Engineering, Isfahan University of Technology, from 1995 to 1997. He is currently a postdoctoral fellow at the Department of Electrical and Computer Engineering, University of Toronto. His research interests include power electronics, distributed generation systems and electric machinery.



Reza Iravani (F'2003) received the B.Sc. degree from Tehran Polytechnic University, Tehran, Iran, in 1976, and the M.Sc. and Ph.D. degrees from the University of Manitoba, Winnipeg, MB, Canada, in 1981 and 1985, respectively, all in electrical engineering. He is currently a Professor at the University of Toronto, ON, Canada. His research interests include power electronics and power system dynamics and control.